Biofouling

The Journal of Bioadhesion and Biofilm Research

ISSN: 0892-7014 (Print) 1029-2454 (Online) Journal homepage: http://www.tandfonline.com/loi/gbif20

Proteins dominate in the surface layers formed on materials exposed to extracellular polymeric substances from bacterial cultures

Yi Yang, Agata J. Wikieł, Leonardo T. Dall'Agnol, Pierre Eloy, Michel J. Genet, José J. G. Moura, Wolfgang Sand, Christine C. Dupont-Gillain & Paul G. Rouxhet

To cite this article: Yi Yang, Agata J. Wikieł, Leonardo T. Dall'Agnol, Pierre Eloy, Michel J. Genet, José J. G. Moura, Wolfgang Sand, Christine C. Dupont-Gillain & Paul G. Rouxhet (2016) Proteins dominate in the surface layers formed on materials exposed to extracellular polymeric substances from bacterial cultures, Biofouling, 32:1, 95-108

To link to this article: http://dx.doi.org/10.1080/08927014.2015.1114609

BIOFOULING, 2016
VOL. 32, NO. 1, 95–108
http://dx.doi.org/10.1080/08927014.2015.1114609

Taylor & Francis
Taylor & Francis Group

Proteins dominate in the surface layers formed on materials exposed to extracellular polymeric substances from bacterial cultures

Yi Yang[a], Agata J. Wikieł[b], Leonardo T. Dall'Agnol[c], Pierre Eloy[a], Michel J. Genet[a], José J. G. Moura[c], Wolfgang Sand[b], Christine C. Dupont-Gillain[a] and Paul G. Rouxhet[a]

[a]Institute of Condensed Matter and Nanoscience (IMCN) – Bio & Soft Matter (BSMA), Université catholique de Louvain, Louvain-la-Neuve, Belgium; [b]Biofilm Centre, Aquatische Biotechnologie, Universität Duisburg – Essen, Essen, Germany; [c]REQUIMTE-CQFB, Departamento de Química, Faculdade de Ciências e Tecnologia, Universidade Nova de Lisboa, Caparica, Portugal

ABSTRACT

The chemical compositions of the surface conditioning layers formed by different types of solutions (from isolated EPS to whole culture media), involving different bacterial strains relevant for biocorrosion were compared, as they may influence the initial step in biofilm formation. Different substrata (polystyrene, glass, steel) were conditioned and analyzed by X-ray photoelectron spectroscopy. Peak decomposition and assignment were validated by correlations between independent spectral data and the ubiquitous presence of organic contaminants on inorganic substrata was taken into account. Proteins or peptides were found to be a major constituent of all conditioning layers and polysaccharides were not present in appreciable concentrations; the proportion of nitrogen which may be due to DNA was lower than 15%. There was no significant difference between the compositions of the adlayers formed from different conditioning solutions, except for the adlayers produced with tightly bound EPS extracted from *D. alaskensis*.

ARTICLE HISTORY
Received 31 July 2015
Accepted 27 October 2015

KEYWORDS
Extracellular polymeric substances (EPS); surface conditioning; biofilms; proteins; X-ray photoelectron spectroscopy (XPS); biocorrosion

Introduction

Biofilms are composed of microbial cells in a matrix which may represent about 90% of the biofilm in dry mass and contains dead cells, cell fragments and extracellular polymeric substances (EPS). The term EPS initially referred to extracellular polysaccharides but nowadays includes also proteins, DNA, lipids and humic substances (Wingender et al. 2001; Conrad et al. 2003; Flemming & Wingender 2003). The composition of the EPS greatly depends on the microbial species and environmental conditions; they are a dynamic system, heterogeneous in composition and changing over time (Flemming & Wingender 2003, 2010). EPS play a major role in the mechanical stability of the biofilm (Flemming 2011). Extracellular DNA has a role in biofilm formation, organization and strength (Whitchurch et al. 2002; Berne et al. 2010; Gloag et al. 2013; Jakubovics et al. 2013). EPS produced by planktonic cells are frequently subject to an operational distinction between loosely bound (LB) and tightly bound (TB). LB-EPS can be obtained by collecting the supernatant of bacterial cultures by centrifugation. TB-EPS, which are more strongly associated to cells, can be extracted in different ways: a mild method involves cation-exchange resins; aggressive methods may cause cell lysis and lead to contamination with intracellular components. The results of Beech, Hanjagsit et al. (1999) showed differences in molecular composition between LB and TB-EPS.

Dissolved organic matter tends to adsorb onto materials placed in natural aqueous environments (Neihof & Loeb 1974; Schneider & Leis 2003). Owing to the respective rates of transport (Boonaert et al. 2002), the immersion of a material in a medium containing biological constituents may lead to surface conditioning by adsorption of macromolecules before an appreciable surface coverage with bacteria takes place. Surface modification by adsorption of EPS, river organic matter, humic substances and model compounds (Dufrêne et al. 1996; Gómez-Suárez et al. 2002; Stadler et al. 2010; Hwang et al. 2012a, 2012b, 2013) was shown to be an important factor influencing bacterial attachment. The influence of extracellular DNA on bacterial adhesion and biofilm formation has been demonstrated (Whitchurch et al. 2002; Swartjes et al. 2013). Modification of surface electrical properties has been a major line of tentative understanding. However, the

CONTACT Paul G. Rouxhet paul.rouxhet@uclouvain.be
The supplemental material for this paper is available online at http://dx.doi.org/10.1080/08927014.2015.1114609.

particular properties of adsorbed macromolecules (steric repulsion, segment attraction, bridging) and specific interactions with the cells may also be involved (Boonaert et al. 2002). EPS may also be directly related to biocorrosion processes (Zinkevich et al. 1996; Beech et al. 1998; Beech, Zinkevich et al. 1999).

Footprints left after the detachment of adhering bacteria were observed by light and electron microscopy, which raised the question of their composition, in comparison with the composition of 'polymers isolated from the culture supernatant or the bacterial cell surface' (Neu & Marshall 1991, p. 101). Surface analysis by X-ray photoelectron spectroscopy (XPS) demonstrated that the chemical composition was similar for the organic layers formed on a substratum in contact with the aqueous phase of a bacterial culture and a substratum submitted to cell sedimentation, adhesion and detachment (Dufrêne et al. 1996).

The composition of conditioning films is quite diverse (Jain & Bhosle 2009) and its determination may be biased by *a priori* selection of the analysis of certain compounds. The analysis of marine conditioning films by wet chemical methods revealed a strong seasonal variation in carbohydrate concentration which followed the variation in seawater (Jain & Bhosle 2009). XPS gives a spectrum of photoelectrons emitted under X-ray irradiation, probes a thin layer (5–10 nm in thickness) at the sample surface and provides concentrations of elements and chemical functions. It is thus a suitable method for providing an overview of the main classes of compounds present in an adsorbed organic layer, which is complementary to information on the surface morphology or the surface distribution of specific compounds (Neu & Marshall 1991; Stadler et al. 2010). XPS was used to check the composition of conditioning layers formed by defined compounds (Hwang et al. 2012a, 2013), but also provided an evaluation of the overall chemical composition of the layers left after bacterial detachment, formed in contact with cell cultures or EPS solutions, or made with organic matter from river water (Dufrêne et al. 1996; Beech et al. 2000; Gómez-Suárez et al. 2002; Hwang et al. 2012a, 2012b; Torres Bautista et al. 2015).

The aim of this work was to compare, by XPS analysis, the chemical natures of conditioning layers formed at the surface of materials as a result of contact with solutions containing EPS related to bacteria. It addresses limitations inherent to the complexity of the systems, distinguishing between oxygen of the organic layer and oxygen of the substrata, and coping with the ubiquitous presence of organic contaminants at the surface of high energy solids. The results presented provide a comparison between different bacterial species of interest in the field of biocorrosion: *Desulfovibrio alaskensis* (Feio et al. 2004) and *Desulfovibrio desulfuricans* (Dall'Agnol et al. 2014) involved in oxygen-free corrosion in the environment, and *Pseudomonas* NCIMB 2021 involved in corrosion in the marine environment (Beech et al. 2000; Yuan & Pehkonen 2007); different types of conditioning solutions, from isolated EPS to whole culture media; and different substrata. Materials were selected to include a hydrophobic model, polystyrene, a hydrophilic model, glass, and two materials relevant to various environmental applications, stainless steel and carbon steel.

Materials and methods

Test solutions

Desulfovibrio desulfuricans (ATCC 27774) was cultured in a vitamin medium, referred to as VMN (Zinkevich & Beech 2000), containing 6 g l^{-1} of lactate and supplemented either with sulfate or nitrate (concentrations given in Supplemental material), in order to compare the two electron acceptors. The base culture medium was deaerated by bubbling with nitrogen gas (20 min for 100 ml of solution) and autoclaved (20 min, 121°C) on preparation day. The vitamin solution was sterilized by filtration (0.22 µm, cellulose membrane from Millipore, Merck, Darmstadt, Germany) and added just before inoculation at a concentration of 0.2%. For XPS analysis, a 24 h preculture was used as inoculum (10% V/V) for 100 ml anaerobic bottles, which were incubated at 30°C for six days, without agitation. The cultures were centrifuged (10,000 g; 15 min, 4°C) and the supernatants were immediately filtered with a 0.22 µm pore size cellulose acetate membrane, providing LB-EPS solutions. These were dialyzed at 4°C with a 3.5 kDa membrane (Spectra/Por, Spectrum Laboratories, Breda, The Netherlands) against distilled water for 16 h with stirring at 100 rpm. The dialysis was continued for additional 24 h at 4°C with stirring at 100 rpm, against distilled water, which was changed three times a day. The volume of water used was at least 25 times greater than the volume of the EPS solution. Phenylmethylsulfonyl fluoride (PMSF) was added to a final concentration of 1 mM as a protease inhibitor. Aliquots were frozen, stored at −20°C and thawed prior to use. For the protein profile characterization, *D. desulfuricans* was grown in 2 l anaerobic bottles for three days at 30°C with magnetic stirring until a cell concentration of at least 10^8 cells ml^{-1} was reached.

Desulfovibrio alaskensis AL1 was isolated from a soured oil well in Purdu Bay, Alaska (Feio et al. 2004). Growth was performed anaerobically with stirring at 100 rpm at 30°C in the VMN medium, containing either 0.6 or 6 g l^{-1} of lactate (referred to as 0.6 and 6 lactate) and complemented with sulfate. The detailed composition is given in the Supplemental material. The chemicals were analytical grade from Sigma-Aldrich (St Louis, MO, USA). After

growth for 72 h, the suspension was centrifuged (9,400 g, 12 min, 4°C). One liter of supernatant was collected and immediately double filtered with 0.22 µm pore size cellulose acetate membrane, providing the solution which contained LB-EPS. TB-EPS were extracted from the cell pellet at 4°C, by a mild process involving the removal of multivalent cations with a cation exchange resin (Dowex® Marathon™C, Na^+ form, 20–50 mesh size supplied by Sigma-Aldrich) (Frølund et al. 1996). In order to use an extraction buffer with an ionic strength and conductivity similar to that of the sample collected, the buffer composition was: 2 mM $Na_2PO_4{\cdot}12H_2O$, 4 mM $NaH_2PO_4{\cdot}H_2O$, 0.34 M NaCl, 1 mM KCl, pH=7.4 (adjusted with NaOH). The proportion was 1 g of resin for 2 ml of extraction buffer. The dialysis of LB-EPS and TB-EPS solutions was performed overnight against flowing deionized water at room temperature, using a 3.5 kDa membrane from Spectra/Por. The dialysis was continued for an additional 48 h at 4°C with stirring at 100 rpm, against deionized water, which was changed three times a day. The volume of water used was at least 25 times greater than the volume of the EPS solution. Aliquots of the solutions were frozen, stored at –20°C and thawed prior to use.

In order to determine the possible cell lysis resulting from EPS extraction from *D. alaskensis*, the 2-keto-3-deoxyoctanate (KDO) concentration was determined using KDO as a standard (Karkhanis et al. 1978). These values were compared with a positive control performed on a defined quantity of cells: 0.5 ml of bacterial suspension and 40 µl of 20% SDS heated at 60°C. This indicated that EPS extraction did not provoke cell lysis levels > 1%.

Pseudomonas NCIMB 2021 (National Collection of Industrial, Food and Marine Bacteria, Aberdeen, UK) was cultured in Difco marine broth 2216 (composition given in Supplemental material). Stored bacterial cells were inoculated on a marine agar 2216 plate at room temperature. A single bacterial colony was selected and cultured in 5 ml of marine broth 2216 for 24 h (room temperature, agitation on a rotary shaker set at 120 rpm), and then sub-cultured in 200 ml of marine broth 2216 (room temperature, agitation on a rotary shaker at 120 rpm). Bacterial supernatants were collected in the middle of the exponential growth phase (optical density at 600 nm, $OD_{600} \cong 1.0$) or in the stationary phase ($OD_{600} \cong 1.8$; three-day cultures), by two successive centrifugations (5,000 g, 5 min; Multifuge X1R centrifuge, Thermo Scientific, Erembodegem, Belgium). The fresh sterilized medium was also used as a test liquid. For certain XPS experiments, the supernatants and the culture medium were ultrafiltered at 4°C to remove salts and small molecules, using a centrifugal membrane (Amicon Ultra/15 centrifugal filter, UFC900308, cut-off 3 kDa, Merck, 4,000 g); the ultrafiltration retentate was added with ultrapure water to reach the original volume.

Single-stranded DNA 'TCATGATTTGTCACTGAACCG' was custom-made by Sigma-Aldrich (reference number SY110400604-032) and will be referred to as DNA-032. Ultrapure water was obtained with the PURELAB Ultra device, purchased from ELGA (Wasquehal, Belgium).

Substrata

Glass disks (Gl) with a diameter of 1.2 cm (Menzel-Gläser, Braunschweig, Germany), were cleaned using 'piranha solution' (7:3 V/V mixture of 97% sulfuric acid and 30% peroxide water, both supplied by VWR BDH Prolabo, Leuven, Belgium) for 30 s, followed by rinsing with ultrapure water and drying under nitrogen flow. They were used immediately after cleaning and represent a model hydrophilic surface, as verified by a water contact angle < 10°, measured using the sessile drop method.

Polystyrene substrata (PS) were prepared by spin coating (3,000 rpm for 30 s) a polystyrene solution (4.3 g l^{-1} in toluene; PS from Sigma-Aldrich, CAS number 9003-53-6) on glass. They were prepared one day before use and represent a model hydrophobic surface, the water contact angle being 90 ± 0.4°.

Stainless steel 304-2R (SS) (Arcelor, Isbergues, France) plates (mass%: 18.10 Cr, 9.10 Ni, 1.11 Mn, 0.24 Mo, 0.36 Si, 0.051 C, 0.024 P, 0.001 S, balance Fe), were 1 cm × 1 cm squares, 1 mm thick, with mirror-like surfaces. After removal of the protective plastic film, the coupons were cleaned three times with acetone in an ultrasonic bath for 15 min. Certain coupons were further submitted to UV/ozone treatment (UVO cleaner, Model No.42-220, Jelight Company, Inc., Irvine, CA, USA) for 15 min just before use; these will be referred to as SS-UVO.

Carbon steel St 37–2 (CS) (S235–JR, from Descours & Cabaud, France) plates (maximum mass%: C 0.2, Mn 1.4, N 0.009, S 0.045, P 0.045), were 1 cm × 1 cm squares, 2 mm thick. The coupons were polished with diamond paste (1 µm final grain size), rinsed with water, then with acetone, dried and stored. Just before use, they were cleaned three times with acetone in an ultrasonic bath for 15 min and submitted to UV/ozone treatment as described for SS.

The water contact angle of the steel surfaces is not relevant owing to adventitious contamination left after solvent cleaning or quickly adsorbed from the surrounding atmosphere (Rouxhet 2013). It is < 10° for SS immediately after UVO cleaning but rises quickly upon exposure to air, reaching values above 50° in a few hours.

XPS analysis

Two kinds of samples were analyzed by XPS: (1) substrata conditioned by solutions, and (2) residues of evaporation of the same solutions. Substratum conditioning was performed by immersion in 0.6 ml of the solution in 24-well plates for 2 h, and rinsing. Rinsing was carried out by performing the following operations three times (which provided in principle dilution by a factor of 43 while avoiding repeated removal from the liquid): adding 1.5 ml of ultrapure water, homogeneous stirring, and removing 1.5 ml of liquid. The coupon was then removed and quickly dried under a nitrogen flow. The carbon steel coupons were conditioned in a glove box flushed with nitrogen in order to avoid prolonged exposure of wet coupons to air. To prepare the residues of evaporation, an aliquot of 100 µl of the liquid was deposited onto glass substrata and left to dry in ambient conditions. This process was repeated another two times to form a layer of residue which was visible to the naked eye.

XPS measurements (one spot analyzed per sample) were carried out with a Kratos Axis Ultra spectrometer (Kratos Analytical, Manchester, UK), using monochromated Al Kα radiation (powered at 10 mA and 15 kV) and an eight-channeltron detector. The SS coupons were isolated from the sample holder with double-sided adhesive tape and charge stabilization was ensured by using the Kratos Axis device. Owing to the magnetic character of carbon steel coupons, they were grounded and the magnetic lens and thus the charge stabilization were off for recording their spectra. The analyzed area was 700 µm × 300 µm. The vacuum in the analysis chamber was ~10^{-6} Pa. The direction of photoelectron collection was perpendicular to the sample surface. Survey spectra were recorded with 160 eV pass energy and the narrow scans with a 40 eV pass energy. In the latter conditions, the full width at half maximum (FWHM) of the Ag $3d_{5/2}$ peak of a standard silver sample was ~0.9 eV. The C 1s peak component due to carbon exclusively bound to carbon and hydrogen [C-(C,H)] was fixed at 284.8 eV to set the binding energy scale. The survey spectrum was recorded on each sample and the individual peaks were recorded at the higher resolution when the element was detected on the survey spectrum. The C 1s peak was always recorded twice, at the beginning and at the end, to check for charge stability and the absence of sample evolution as a function of time.

Quantification was carried out with the CasaXPS program (Casa Software Ltd, Abbotskerswell, UK) after linear background subtraction and peak area normalization on the basis of acquisition parameters, using experimental sensitivity factors and transmission factors given by the manufacturer. This provided elemental mole fractions, excluding hydrogen which is not detected by XPS. The C 1s, O 1s and N 1s peaks were decomposed using a Gaussian/Lorentzian (70/30) product function. Further details on peak decomposition are given below.

Characterization of the solutions

The protein and sugar concentrations of the EPS solutions from *D. alaskensis* and *D. desulfuricans* were determined using colorimetric methods (Dubois et al. 1956; Bradford 1976, respectively). The DNA concentration was determined using Burton's (1956) protocol.

One-dimensional polyacrylamide gel electrophoresis was performed on 10% SDS-PAGE using a Mini-Protean 1-D cell from Biorad (Temse, Belgium) according to the method of Laemmli (1970). The proteins were stained for visualization with Coomassie blue (Dyballa & Metzger 2009) or with silver nitrate solution (GE Healthcare 2004). Details on sample preparation are given in Supplemental material (Section 2).

Results

Solutions

The concentrations of proteins, sugars and DNA in solutions of EPS from *D. alaskensis* and *D. desulfuricans* are given in Table 1. The DNA concentrations in the EPS solutions from *D. alaskensis* were too low to provide reliable results. Polyacrylamide gel electrophoresis (PAGE) indicated the presence of numerous proteins in the range of 15 to 250 kDa, with a molar mass distribution which varied appreciably according to the system. No protein was detected by PAGE in the fresh culture medium of

Table 1. Composition of the solutions used for substratum conditioning: concentration (µg ml^{-1}) of proteins, sugars and DNA.

Solutions	Proteins	Sugars	DNA
EPS from *D. alaskensis*, dialyzed			
Loosely bound, 0.6 lactate	1.9	6.7	0.28
Loosely bound, 6 lactate	5.2	6.5	0.23
Tightly bound, 0.6 lactate	173	18	0.17
Tightly bound, 6 lactate	269	65	0.32
EPS from *D. desulfuricans*, dialyzed			
Loosely bound, sulfate	0.34	1.7	
Loosely bound, nitrate	2.3	5.4	

Table 2. Overview of the samples analyzed by XPS: residues of evaporation of conditioning solutions and of DNA solution, substrata (polystyrene, glass, UVO-cleaned and acetone-cleaned SS, CS) before and after conditioning with the solutions.

		Substrata				
Solutions	Evaporation residue	PS	GI	SS-UVO	SS-acet	CS
None		x	x	x		x
EPS from *D. alaskensis*						
Loosely bound, 0.6 lactate, non-dialyzed						x
Loosely bound, 6 lactate, non-dialyzed						x
Loosely bound, 0.6 lactate, dialyzed	x	x	x			x
Loosely bound, 6 lactate, dialyzed	x	x	x			x
Tightly bound, 0.6 lactate, dialyzed	x	x	x			x
Tightly bound, 6 lactate, dialyzed	x	x	x			x
EPS from *D. desulfuricans*						
Loosely bound, sulfate, dialyzed		x	x	x	x	
Loosely bound, nitrate, dialyzed		x	x	x	x	
Solutions related to *Pseudomonas* NCIMB 2021						
Fresh medium non-ultrafiltered		x	x	x	x	
Fresh medium ultrafiltered	x	x	x	x	x	
Supernatant exponential, non-ultrafiltered		x	x	x	x	
Supernatant exponential, ultrafiltered	x	x	x	x	x	
Supernatant stationary, non-ultrafiltered		x	x	x	x	
Supernatant stationary, ultrafiltered	x	x	x	x	x	
DNA-032	x					

Pseudomonas NCIMB 2021. Details are presented in the Supplemental material (Section 2). These results show that the conditioning solutions cover a wide range of protein or protein fragment concentrations and molar masses.

Raw XPS data

The samples analyzed by XPS are presented in Table 2 in a matrix showing the solutions used for the different samples (residues of evaporation and conditioned substrata). The elemental compositions determined by XPS are listed in Supplemental material (Tables S3 to S7); the data are identified by the element, the approximate binding energy of the photoelectrons collected in the peak and the assigned energy level. Fe in steel samples was quantified with the Fe $2p_{3/2}$ component, using a linear baseline as shown previously (Landoulsi et al. 2008). The non-conditioned glass and steel substrata showed carbon concentrations of 12% and ~40%, respectively. This was attributed to organic contaminants which may originate from material processing, from artifacts due to sample preparation, or from contamination by adsorption from the surroundings (either the ambient atmosphere or the spectrometer vacuum chamber). The higher carbon concentration on steel compared to glass is a frequent observation (Rouxhet 2013). The position of the weak S 2p peak varied in the range 162 to 169 eV, depending on the relative importance of sulfur from proteins and sulfate from residual salts. The N/C molar ratio measured on conditioned glass, SS and CS varied between 0.02 and 0.20, thus covering the range between the low values reported for Cu-Ni alloy and the high values reported for SS, both conditioned with EPS from *Pseudomonas* NCIMB 2021 (Beech et al. 2000; Torres Bautista et al. 2015).

Figure 1 presents the range of shapes observed for O 1s, N 1s and C 1s peaks. The binding energy of photoelectrons is influenced by the electron density on the atom, therefore the shape of the peaks results from the superposition of components which are typical of the chemical functions in which the atom is involved. These peaks were decomposed on the basis of previous work with constraints ensuring the consistency required to make quantitative comparison between samples (Genet et al. 2008; Landoulsi et al. 2008; Rouxhet et al. 2008; Rouxhet & Genet 2011). The imposed constraints, the assignment of the components to chemical functions and details regarding peak components (binding energy, FWHM) are given in Table 3. The results of peak decompositions are presented in Tables S3 to S7. The decomposition of the O 1s peaks of glass and carbon steel samples was not performed owing to the overlap of inorganic oxides or hydroxides and organic compounds.

The N 1s peak of the samples of interest was quite different from that of nucleotides, as shown in Figure 1f for single-stranded DNA-032. An evaluation of the upper limit of the DNA contribution to the N 1s peak of evaporation residues and conditioned substrata was performed, based on two independent spectral datasets: the P/N ratio and the shape of the N 1s peak. This is presented in detail in Supplemental material (Section 4) and shows that DNA may not account for > 15% of the total nitrogen.

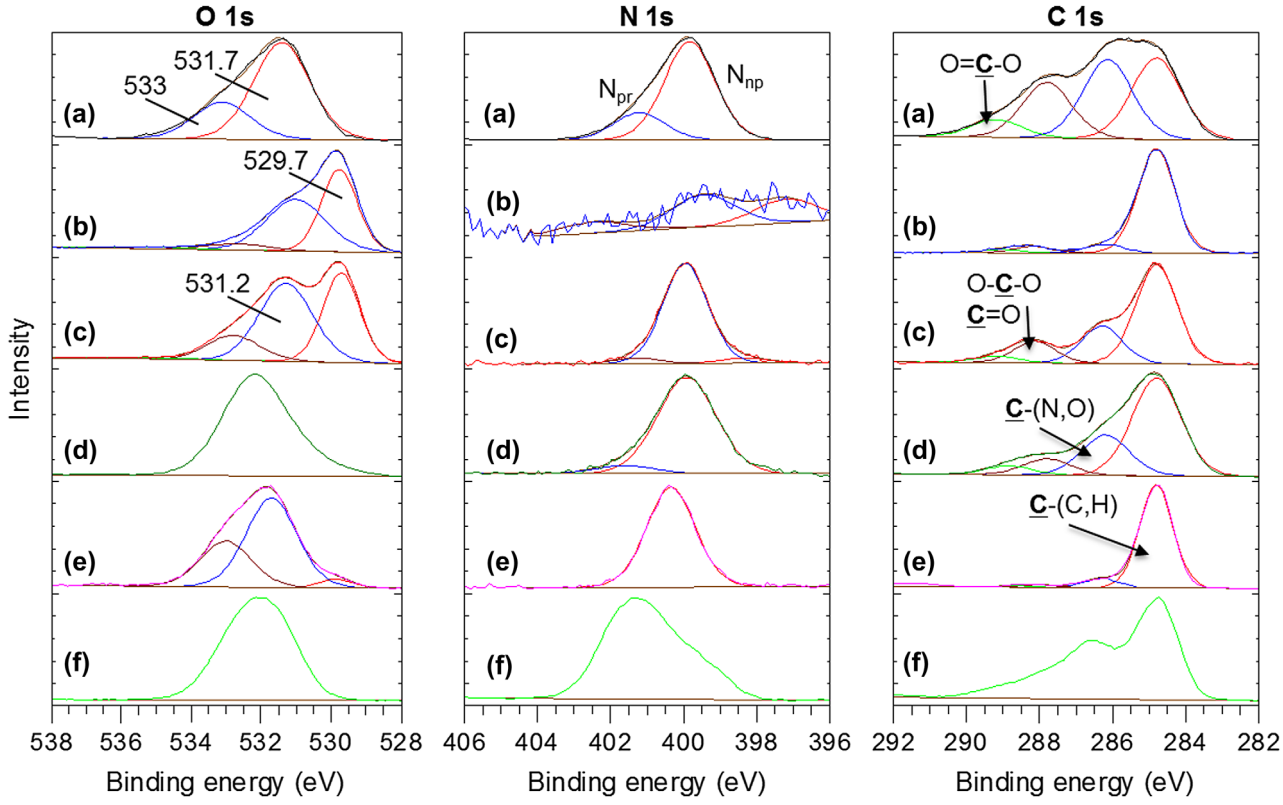

Figure 1. Representative XPS peaks recorded on (a) residue of evaporation of a solution of tightly bound EPS from 0.6 lactate culture after dialysis; (b) SS cleaned with UVO; (c) SS-UVO, (d) GI and (e) PS, each conditioned with the supernatant collected in the stationary phase of *Pseudomonas* NCIMB 2021; and on (f) the residue of evaporation of a solution of DNA-032. Peak decomposition and component position or assignment when reliable. N_{np} = non protonated nitrogen; N_{pr} = protonated nitrogen.

Table 3. Characteristics and assignment of XPS peak components.

Peak / sample	Notation and binding energy (eV)		Assignment	
C 1s / All	$C_{284.8}$	284.8 (a, b)	***C***-(C,H)	Hydrocarbon
	$C_{286.2}$	286.1–286.3 (b)	***C***-(O,N)	Alcohol, amide, amine
	C_{288}	Near 288.0 (b)	O-***C***-O; N=***C***-O	Acetal; amide
	C_{289}	288.8–289.2 (b)	O=***C***-O	Carboxyl, ester
C 1s / Polystyrene		Near 291.5	Shake up of polystyrene	
O 1s / Evaporation residue and polystyrene	$O_{531.5}$	531.2–531.8 (c)	***O***=C (d)	Amide, carboxyl, ester
	O_{533}	Near 533 (c)	***O***-C; C-***O***-C	Alcohol, carboxyl, ester; Ether
O 1s / SS	—	529.7 (e)	Metal oxide	
	$O_{531.5}$	Near 531.2 (f)	Metal hydroxide	
			O=C	Amide, carboxyl, ester
	O_{533}	Near 532.8 (f)	***O***-C; C-***O***-C	Alcohol, carboxyl, ester; Ether
N 1s / All	N_{np}	399.8–400.2 (g)		Amine, amide
	N_{pr}	> 401 (g)		Protonated amine
N 1s / Steel	—	< 398.5	Reduced form of N, Mo $3p_{1/2}$	

(a) Fixed at 284.8 eV to set the binding energy scale.
(b) FWHM imposed to be the same for the four components of a C 1s peak; found by best fitting to be between 1.2 and 1.5 eV for inorganic substrata, close to 1.2 eV for polystyrene substrata and between 1.3 and 1.6 eV for evaporation residues.
(c) FWHM imposed to be the same for these two components and found to be between 1.6 and 2.0 eV.
(d) With a possible small contribution of inorganic salts.
(e) Component drawn according to the low binding energy edge of the peak without constraint regarding FWHM.
(f) FWHM imposed to be the same for these two components and found to be between 1.8 and 2.0 eV.
(g) FWHM imposed to be the same for these two components and found to be between 1.3 and 2.0 eV.

Correlations between XPS data

While the consistency required for comparison between samples is ensured by imposing constraints, peak decomposition is an interpretative approach which involves a trade-off between constraints imposed and information generated (Rouxhet & Genet 2011; Touré et al. 2014). Correlations between spectral data of different character (elemental concentrations, peak shapes) were used

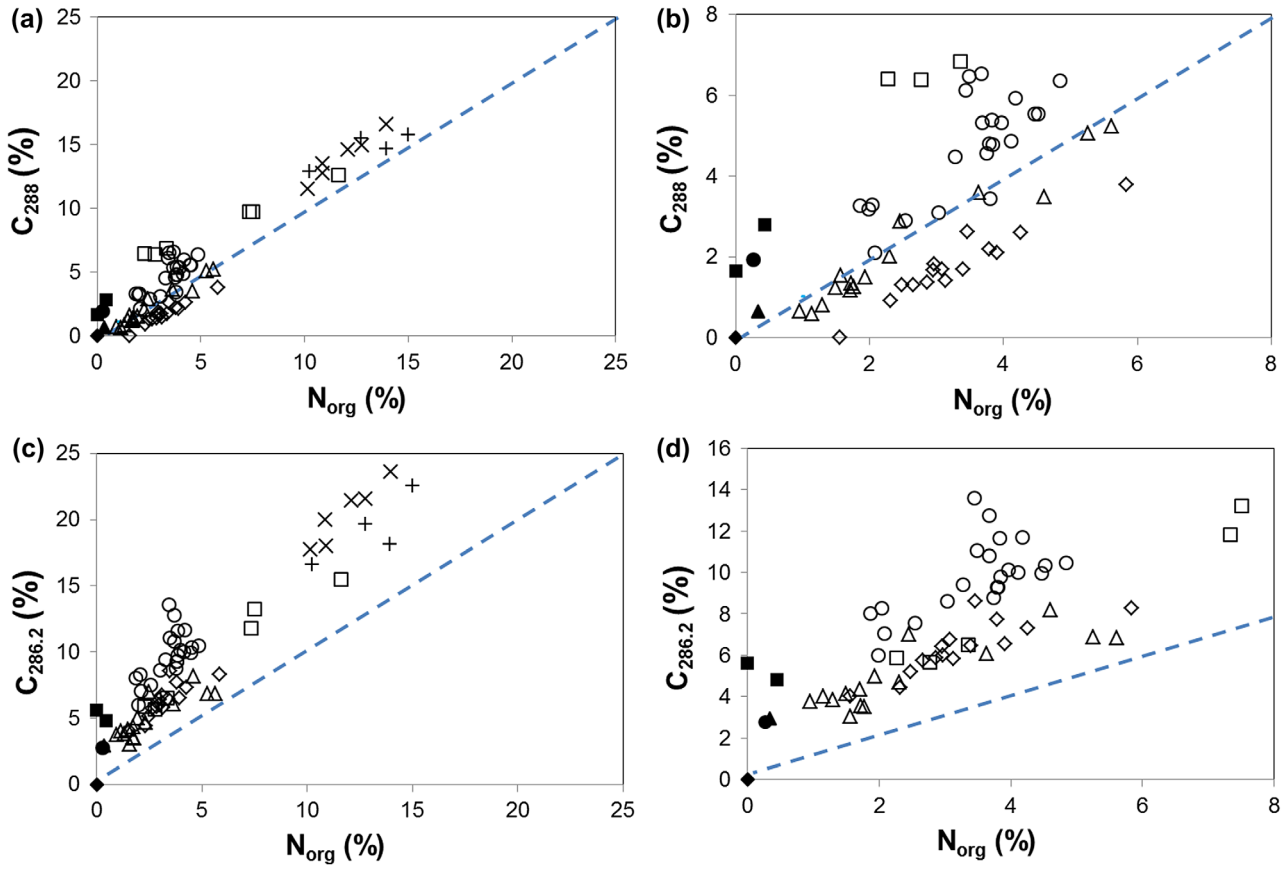

Figure 2. Plot of the molar concentrations associated to C 1s peak components (C_{288} in a and b; $C_{286.2}$ in c and d), *vs* the organic nitrogen concentration (N_{org}) determined by XPS: residues of evaporation of EPS solutions from *D. alaskensis* (+), and of *Pseudomonas* NCIMB 2021 related solutions (×); non-conditioned Gl (▲), PS (♦), SS (●) and CS (■); Gl (Δ), PS (◊), SS (○) and CS (□) conditioned with the various solutions. Note that (b) and (d) are zooms of (a) and (c), respectively. Broken line, 1:1 relation expected for amide.

to evaluate the significance (relevance and limitation) of peak decomposition and of the results obtained, as performed previously (Ahimou et al. 2007; Genet et al. 2008; Rouxhet et al. 2008; Aguié-Béghin et al. 2009; Rouxhet & Genet 2011). Figure 2a presents the plot of the concentration of carbon responsible for the component close to 288.0 eV, C_{288}, as a function of the concentration of organic nitrogen, N_{org}. A zoom of Figure 2a is shown in Figure 2b. Figure 2c (zoom in Figure 2d), presents the plot of the concentration of carbon responsible for the C 1s component at 286.1–286.3 eV, noted $C_{286.2}$, as a function of N_{org}. The trends were close to a 1:1 relationship, which is expected for the amide function [HC-NH-(C=O)], forming the backbone of proteins. More precisely, ratios of 0.84 and 1.04 are expected for C_{288}/N_{org} and $C_{286.2}/N_{org}$, respectively, from computations based on the amino-acid composition of bovine serum albumin (BSA), taken as a model protein (Touré et al. 2014). The upward deviation shown by evaporation residues is higher for $C_{286.2}/N_{org}$ compared to C_{288}/N_{org}, and is attributed to the presence of polysaccharides, responsible for C-***C***-O and O-***C***-O contributions, with a ratio C-***C***-O / O-***C***-O of 5. For polystyrene (Figure 2b and d, diamond symbols), the upward deviation of $C_{286.2}/N$ was concomitant with a downward deviation of C_{288}/N. This suggests that decomposition of the C 1s peak, with a high intensity of the component at 284.8 eV, may systematically underestimate the 288 eV component and overestimate the 286.2 eV component, as observed for BSA conditioned polystyrene (Touré et al. 2014). For the steel samples (circles, squares) both the C_{288}/N and $C_{286.2}/N$ experimental ratios were above the values expected for proteins, not only for conditioned substrata but also for non-conditioned substrata. This revealed the presence of oxidized carbon which was not in the form of amide and may be due to polysaccharides or oxygen-containing organic contaminants. Glass substrata (triangles) showed a behavior intermediate between polystyrene and steel.

Figure 3a shows that the concentration of $O_{531.5}$ was very close to that of N_{org} for polystyrene samples, in agreement with the presence of amide in the adsorbed phase. It was slightly higher for evaporation residues owing to a contribution of salts (presence of phosphate, sulfate, Si, B, Al; see Table S3). In contrast, the concentration of $O_{531.5}$

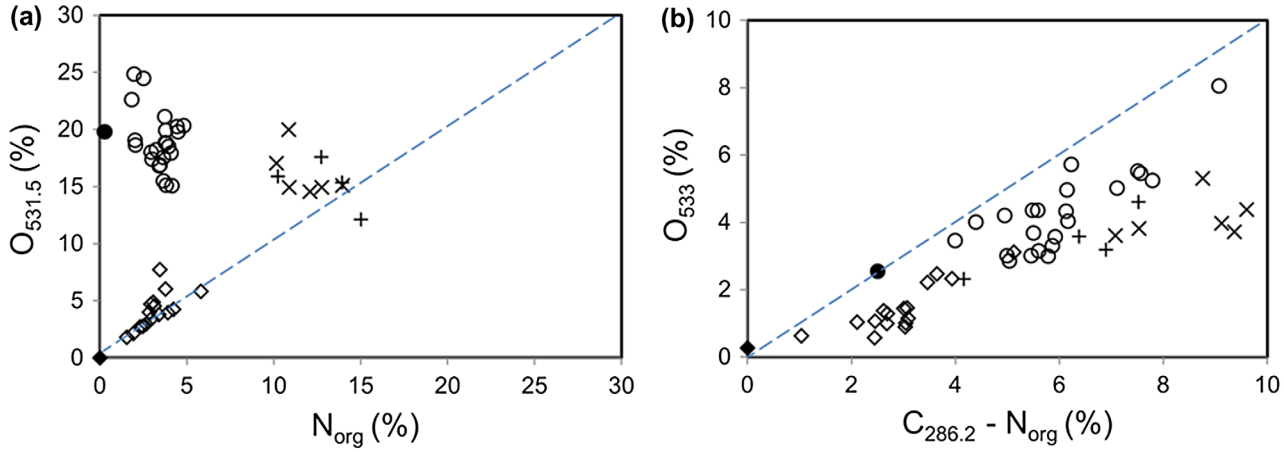

Figure 3. Plot of molar concentrations determined by XPS: (a) $O_{531.5}$ *vs* N_{org} and (b) O_{533} *vs* ($C_{286.2}$ – N_{org}). Residues of evaporation of EPS solutions from *D. alaskensis* (+), and of *Pseudomonas* NCIMB 2021 related solutions (×); non-conditioned PS (♦) and SS (●); PS (◊) and SS (○) conditioned with the various solutions. Broken line, 1:1 relation expected for amide in (a) and for alcohol, ester and polysaccharide in (b).

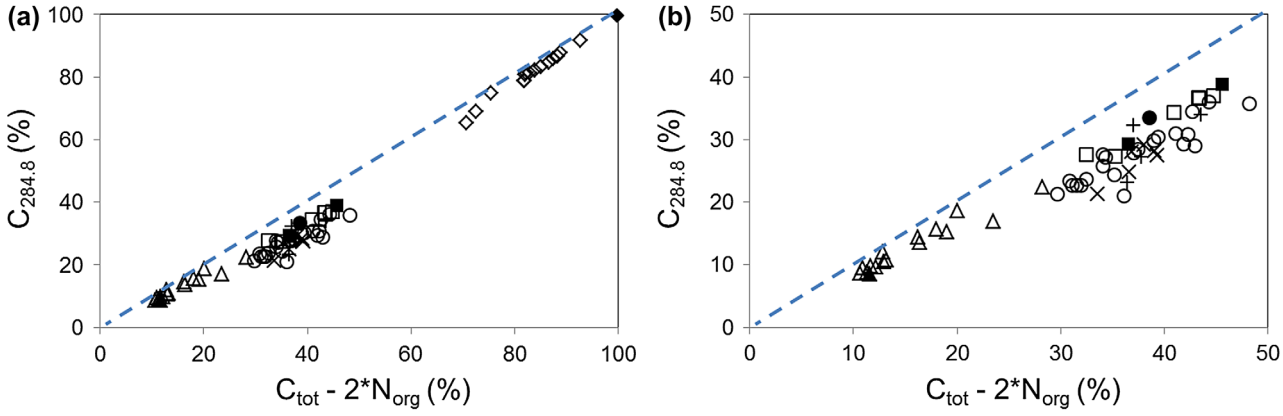

Figure 4. Plot of the molar concentrations of $C_{284.8}$ *vs* (C_{tot} – 2×N_{org}) determined by XPS: residues of evaporation of EPS solutions from *D. alaskensis* (+), and of *Pseudomonas* NCIMB 2021 related solutions (×); non-conditioned glass (▲), PS (♦), SS (●) and CS (■); glass (△), PS (◊), SS (○) and CS (□) conditioned with the various solutions. Note that (b) is a zoom of (a). Broken line, 1:1 relation expected if only hydrocarbons and amide functions were present.

was much higher than that of N_{org} for SS samples, owing to the overlapping contribution of metal hydroxide.

Figure 3b presents the plot of the concentration of O_{533} *vs* ($C_{286.2}$ – N_{org}). Here, N_{org} was subtracted from $C_{286.2}$ to remove the contribution of amide functions. A 1:1 relationship may be expected for alcohol (***C***-***O***H), ester (***C***-***O***-C=O) and non-substituted polysaccharide [three moieties ***C***-***O***-H, 2 C-***O***-C and 2 C-***C***-O per repeat unit). The correlation coefficient was 0.89 for the collection of polystyrene and SS samples and 0.68 if evaporated residues were added to this collection.

The correlations discussed above support the chemical relevance of the spectral data. However, the scatter in the graphs and systematic deviations with respect to values expected for chemical models pointed to the low precision of the O 1s peak decomposition and to a possible underestimation of $C_{286.2}$. Figures 2a and 3a clearly show the importance of amide functions at the surface of evaporation residues and of conditioned substrata. In N-acetylated amino sugars and in proteins, the amide function has the structural formula [HC-NH-(C=O)]. Designating the total carbon concentration by C_{tot}, (C_{tot} – 2×N_{org}) represents carbon which is not in the form of amide (if all N_{org} is attributed to amide). On the other hand, the C 1s component at 284.8 eV, $C_{284.8}$, is due to carbon only bound to carbon and hydrogen (hydrocarbon function, typical of lipids and side chains of proteins). Figure 4 presents the plot of $C_{284.8}$ *vs* (C_{tot} – 2×N_{org}). All the data were distributed along a bow shape, the ends being close to the 1:1 relationship. The data for polystyrene samples were located at the high end but were not informative owing to the strong contribution of the substratum. The

deviations with respect to the 1:1 relationship reflected the concentration of carbon which was neither in a form of hydrocarbon function, nor in the form of amide. This was much lower for glass samples than for steel samples, both for bare and conditioned substrata, which indicated a difference between the two types of substrata regarding organic contaminants.

Discussion

Composition of the adlayer

The composition of the organic adlayers is often expressed by the molar concentration ratios of elements (Beech et al. 2000; Torres Bautista et al. 2015). An expression in terms of mass concentration of organic compounds is much more explicit but is made difficult by the complexity of the biochemical compounds and by the presence of organic contaminants (Touré et al. 2014). According to the correlations presented in Figures 2 and 3, amide moieties are important constituents and can be quantified by using nitrogen as a marker. This neglects the part of nitrogen in the form of DNA, demonstrated to be in low concentration. In previous reports on the surface analysis of microbial cells and conditioning layers, nitrogen was also attributed to amide and was considered as a marker for proteins (Dufrêne et al. 1996; Gómez-Suárez et al. 2002; Genet et al. 2008; Rouxhet & Genet 2011; Hwang et al. 2013). Accordingly, the surface composition was modeled in terms of proteins, polysaccharides and hydrocarbons. However, polysaccharides frequently contain N-acetylated amino sugars in which nitrogen is also in the form of amide. For this reason and also in order to cope with surface contaminants, the surface composition was modeled here on other bases.

Figure 4 shows that carbon which is not in the form of amide ($C_{tot} - 2{\times}N_{org}$) may be separated into two categories: carbon only bound to carbon and hydrogen ($C_{284.8}$), and oxidized carbon in addition to the carbon present in the form of amide ($C_{add} = C_{tot} - 2{\times}N_{org} - C_{284.8} = C_{ox} - 2{\times}N_{org}$ where $C_{ox} = C_{286.2} + C_{288.0} + C_{289}$). The advantage of basing the quantification on C_{ox} is that it is not affected by the uncertainty of the decomposition between the 286.2 and 288 eV components. Note that the component at 289 eV is very weak and its influence on the final results is not significant. For many organic functions (alcohol, primary amide or amine, ester, aldehyde, ketone), and mostly for those which are relevant in biosystems, $C_{ox} = O_{org} + N_{org}$. An exception is the case of ether functions, for example ($C_{ox}/O_{org} = 2$), which is responsible for a ratio $C_{ox}/O_{org} = 1.2$ of non-chemically modified polysaccharides. Another exception is the case of carboxylic acid or carboxylate functions, for which $C_{ox}/O_{org} = 0.5$. As discussed above, the oxygen due to the organic layer adsorbed on an inorganic oxide substratum often cannot be distinguished from the oxygen of the substratum. However, the concentration of organic oxygen may be approximated by $O_{org} = C_{ox} - N_{org}$ (Landoulsi et al. 2008, 2011).

The composition of the adlayers and of the surface of evaporation residues was thus expressed in terms of four chemical entities: amide [HC-NH-(C=O)] quantified by N, CH_2 quantified by $C_{284.8}$, additional carbon quantified by $C_{add}=C_{ox} - 2{\times}N_{org}$ and additional organic oxygen quantified by $O_{add}=O_{org} - N_{org} = C_{ox} - 2^*N_{org}$. The molar concentrations of the elements used as markers were converted into the weight percentage of the corresponding chemical entities (g per 100 g of evaporation residue or organic adlayer), using the molar mass of these entities as explained in the Supplemental material (Section 5). While this procedure involves approximations, its reliability is demonstrated by the application to BSA, based on its amino-acid composition (Toure et al. 2014), which provides a molar mass of 63,085 Da, to be compared with the real molar mass equal to 66,464 Da. The results of the computations are given in Table 4. The discussion below is based on the composition of the adlayer expressed as weight % of amide [HC-NH-(C=O)], CH_2 and sum $C_{add} + O_{add}$. If the sum of C_{add} and O_{add} is due to non-chemically modified polysaccharide, the molar concentration of O_{add} should be $C_{add}/1.2 = [C_{ox} - 2{\times}N_{org}]/1.2$, instead of $[C_{ox} - 2{\times}N_{org}]$. In practice, neglecting the 1.2 ratio leads to a satisfactory evaluation of the weight of polysaccharides, as an entity composed of six C atoms and six O atoms weighs 168 g, which is close to the weight of one repeat unit $C_6H_{10}O_5$ equal to 162 g.

The weight percentages of the three moieties considered are presented in Figure 5 in the form of ternary composition diagrams (Graham & Midgley 2000), the corners of which represent 100 wt % of amide (pole relevant for proteins and N-acetylated functions of polysaccharides), 100 wt % CH_2 (pole typical of lipids and protein side chains) and 100 wt % $C_{add} + O_{add}$ (pole representative of oxidized organic compounds, including polysaccharides). As an example the closed triangle representing the data computed for BSA (Figure 5) corresponds to 69.3% amide, 30.3% CH_2, 0.4% ($C_{add} + O_{add}$). The figure presents the results for evaporation residues and each substratum in a distinct diagram, while the symbols allow the different types of conditioning solutions to be distinguished.

Figure 5a shows that all evaporation residues fall close together and differ from BSA, by a proportion of 20% ($C_{add} + O_{add}$) which may be due to contaminants or to other compounds containing oxidized carbon, presumably polysaccharides. The surface of evaporation residues was thus mainly composed of proteins or protein fragments. Note that proteins tend to accumulate at the liquid–air interface which generates the analyzed evaporation residue surface,

Table 4. Global results of the XPS analysis of residues of evaporation and of substrata conditioned with the solutions: mass proportion of the model moieties amide [HC-NH-(C=O)], CH_2, additional carbon C_{add} and additional organic oxygen O_{add} in the organic adlayer; sum of the mole fractions $C_{tot} + C_{ox}$ (%)*.

Sample		Proportion in adlayer (weight %)				$C_{tot} + C_{ox}$
		Amide	CH_2	C_{add}	O_{add}	Mole fraction (%)
Evaporation residues	EPS from *D. alaskensis*, dialyzed					
	Loosely bound, 0.6 lactate	51.3	27.4	9.1	12.2	99.4
	Loosely bound, 6 lactate	43.5	36.0	8.8	11.7	94.2
	Tightly bound, 0.6 lactate	54.7	21.1	10.4	13.8	109.9
	Tightly bound, 6 lactate	57.1	33.0	4.3	5.7	97.7
	Solutions related to *Pseudomonas* NCIMB 2021, ultrafiltered					
	Fresh medium	47.0	32.4	8.8	11.8	86.4
	Fresh medium	48.1	32.2	8.4	11.2	90.6
	Supernatant exponential phase	48.6	27.5	10.3	13.7	99.5
	Supernatant exponential phase	54.9	21.0	10.3	13.7	101.6
	Supernatant stationary phase	50.6	27.8	9.3	12.3	101.1
	Supernatant stationary phase	47.3	27.1	11.0	14.6	91.8
Glass	Not conditioned	8.4	53.1	16.5	22.0	16.0
	Conditioned with EPS from *D. alaskensis*, dialyzed					
	Loosely bound, 0.6 lactate	27.6	57.9	6.2	8.3	25.0
	Loosely bound, 6 lactate	33.6	50.8	6.7	8.9	18.6
	Tightly bound, 0.6 lactate	49.4	43.8	2.9	3.8	42.5
	Tightly bound, 6 lactate	62.1	33.2	2.0	2.7	36.2
	Conditioned with EPS from *D. desulfuricans*, dialyzed					
	Loosely bound, sulfate	21.6	50.2	12.1	16.1	17.6
	Loosely bound, nitrate	29.0	48.3	9.7	12.9	17.9
	Conditioned with solutions related to *Pseudomonas* NCIMB 2021					
	Fresh medium, as such	34.4	47.5	7.8	10.4	20.6
	Fresh medium, as such	41.5	44.7	5.9	7.9	35.0
	Fresh medium, ultrafiltered	27.7	50.1	9.5	12.7	21.6
	Supernatant exponential, as such	32.4	47.7	8.5	11.4	28.4
	Supernatant exponential, as such	35.1	42.9	9.4	12.5	52.4
	Supernatant exponential, ultrafiltered	30.9	47.5	9.3	12.3	22.2
	Supernatant stationary, as such	24.6	42.6	14.0	18.7	39.8
	Supernatant stationary, as such	25.4	50.3	10.4	13.9	30.4
	Supernatant stationary, ultrafiltered	23.6	49.7	11.5	15.3	19.4
Carbon steel	Not conditioned	0.0	66.9	14.2	18.9	43.8
		3.3	71.9	10.7	14.2	54.1
	Conditioned with EPS from *D. alaskensis*					
	Loosely bound, 0.6 lactate, dialyzed	14.7	60.1	10.8	14.3	61.6
	Loosely bound, 0.6 lactate, non-dial	18.2	60.5	9.1	12.2	60.8
	Loosely bound, 6 lactate, dialyzed	22.0	56.3	9.3	12.4	61.0
	Loosely bound, 6 lactate, non-dial	36.9	45.9	7.4	9.8	79.6
	Tightly bound, 0.6 lactate, dialyzed	41.0	37.3	9.3	12.4	73.3
	Tightly bound, 6 lactate, dialyzed	55.4	33.0	5.0	6.6	83.8

*Evaluation of the sum of carbon, organic oxygen and organic nitrogen mole fractions (% with respect to all elements except hydrogen).

as observed for food products and pharmaceutical preparations. (Bosquillon et al. 2004; Rouxhet & Genet 2011).

Non-conditioned glass (Figure 5b) showed 40% ($C_{add} + O_{add}$) and 50% CH_2 due to organic contaminants. Conditioning glass introduced proteins and decreased appreciably the relative concentration of oxidized carbon which was not in the form of amide. The influence of the nature of the conditioning solution was not significant except for TB-EPS solution of *D. alaskensis*, which brought the adlayer composition much closer to that of pure protein. The polystyrene samples are not presented in Figure 5, owing to the dominant contribution of CH_2 due to the substratum. However, Table 4 shows that the amide proportion in the zone probed by XPS was about twice larger after conditioning with TB-EPS compared to LB-EPS.

SS treated with UV-ozone and non-conditioned (Figure 5c) showed ~25% of ($C_{add} + O_{add}$) and 75% CH_2, which were due to organic contaminants. After conditioning with any solution, samples were clustered in a narrow domain of composition, without any significant difference between samples cleaned with acetone and samples treated with UV-ozone. While substratum conditioning shifted the adlayer composition by bringing 15 to 30% amide, the increase of $C_{add} + O_{add}$ was only ~10%, which indicated that proteins were dominating among the adsorbed compounds compared to polysaccharides, amino-acetylated or not. The major contribution of protein in the conditioning layer formed on Cu-Ni alloy by EPS from *Pseudomonas* NCIMB 2021 was also revealed by the similarity with the alloy conditioned with BSA regarding the N/C ratio and the C 1s peak shape (Torres Bautista et al. 2015).

CS (Figure 5d) showed a contaminant composition similar to that of SS. Conditioning with EPS of *D. alaskensis* markedly shifted the adlayer composition

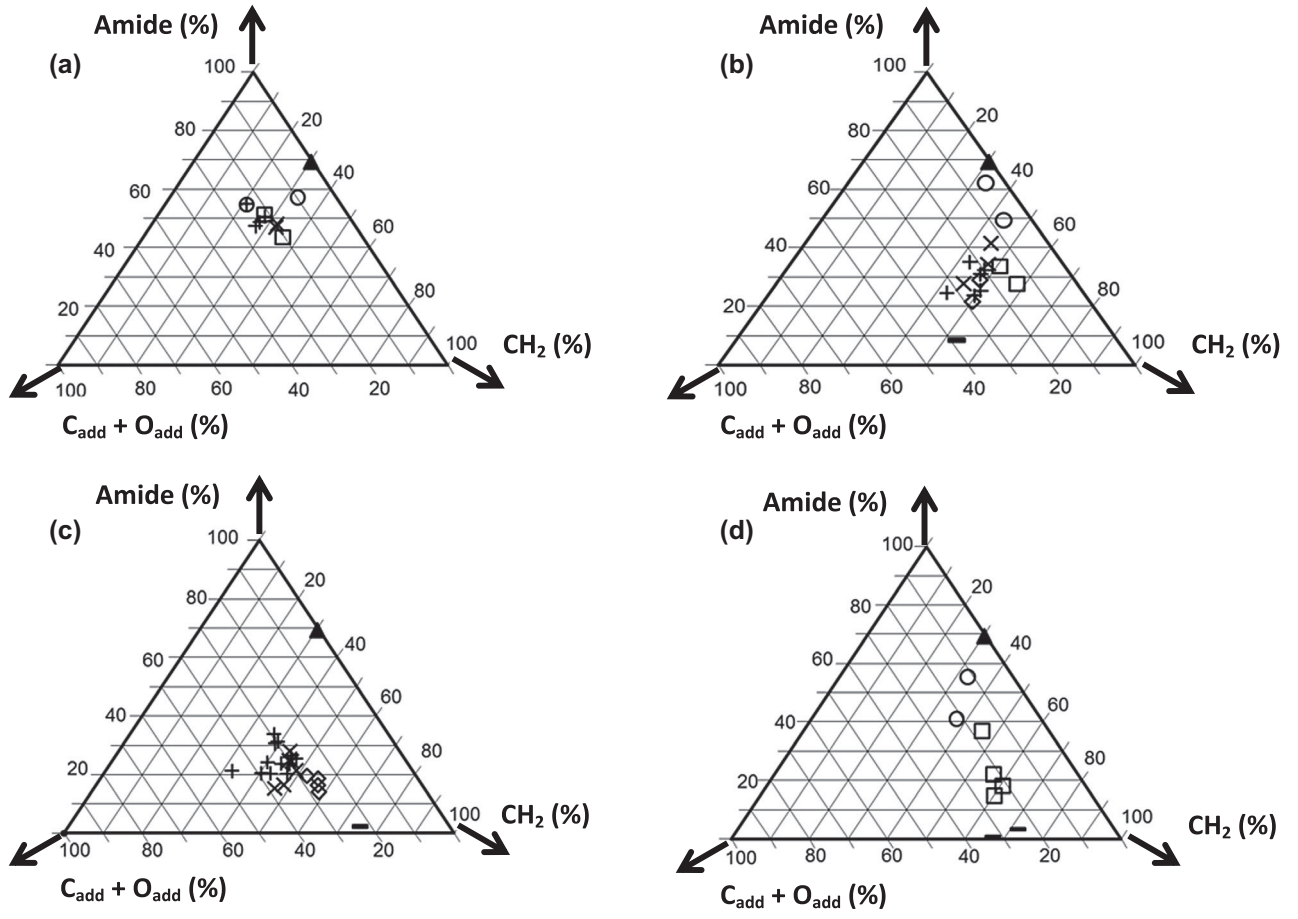

Figure 5. Mass concentration of amide (HC-NH-C=O), hydrocarbon CH_2 and additional carbon and oxygen (C_{add}+O_{add}) determined by XPS on (a) residues of evaporation; (b) glass, (c) SS and (d) CS, either not conditioned (-), conditioned with tightly bound EPS from *D. alaskensis* (○), conditioned with loosely bound EPS from *D. alaskensis* (□) or *D. desulfuricans* (◊), and conditioned with fresh culture medium (×) or supernatants of cultures of *Pseudomonas* NCIMB 2021 (+). Computed value for BSA (▲).

towards the amide pole without any increase in oxygenated compounds, revealing a notable uptake of proteins. It is noteworthy that, as observed on glass and polystyrene, TB-EPS led to a higher protein concentration, compared to LB-EPS. The higher protein concentration after conditioning with TB-EPS compared to LB-EPS was in agreement with the results reported by Beech et al. (2000). Solutions of TB-EPS showed a much higher protein/sugar concentration ratio (Table 1) compared with solutions of LB-EPS.

Nitrogen was entirely assigned to amide in the computations providing Figure 5. If 15% of nitrogen is due to DNA instead of protein, the coordinates of points along the amide axis should be shifted by a factor of 0.85, which has only a marginal influence compared to the difference observed between the sets of samples. The possible impact of DNA may also be determined by considering that one mole of N corresponds to 56 g of amide moieties [HC-NH-(C=O)], 85 g of protein (BSA taken as model) and 82 g DNA (ATGC taken as model). If the concentration of DNA was appreciable, the composition could be modeled in terms of the same variables plus DNA. For that purpose, the N 1s peak could be separated into two components to discriminate between amide of protein and DNA. However, to be accurate, this should rely on a more systematic comparison of the spectra of representative proteins and of DNA.

Adlayer thickness

The description of the organic adlayer present on the substrata, as presented in Figure 5, should ideally include the evaluation of its thickness (Landoulsi et al. 2011). This would require simulations based on models of the adsorbed layer involving hypothetical degrees of coverage and layer thicknesses and would not be reliable owing to the complexity of the adsorbed layer and the lack of XPS measurements at different photoelectron collection angles. However, comparison of adsorbed amounts was made between samples with the same substratum. This was based on the mole fraction of C_{tot} + C_{ox} provided by the XPS analysis, as it was an evaluation of the sum

of concentrations $C_{tot} + O_{org} + N_{org}$, and thus reflected the contribution of the adlayer to the XPS spectrum. The results are presented in Table 4 (last column). The computation for polystyrene samples was not relevant, owing to the contribution of the substratum to the carbon peak. Conditioning substrata with the solutions only moderately increased the contribution of the adlayer to the XPS spectrum (factor 1–2 for glass, about 1.5 for CS, 1–1.5 for UVO treated SS), and thus its thickness, while it changed its composition, essentially by bringing proteins to the surface. Comparison between different liquids indicated a rather high variability in $C_{tot} + C_{ox}$. It did not reveal any significant difference in the adsorbed layer thickness between the LB-EPS of *D. alaskensis* or *D. desulfuricans*, on the one hand, and fresh or spent culture media of *Pseudomonas* NCIMB 2021, on the other hand. The significance of the higher values found for TB-EPS compared to LB-EPS (glass and CS substrata) is possible, but not established, owing to the small number of samples. If the SS substratum is assumed to be perfectly smooth and if the adlayer is assumed to be homogeneous with a constant thickness, mole fractions of $C_{tot} + C_{ox}$ in the range of 50 to 60% correspond to adlayer thicknesses of the order of 3 nm (Landoulsi et al. 2011).

A comparison between the substrata in Figure 5 reveals interesting differences. For glass, conditioning decreased the percentage of $C_{add} + O_{add}$, which was attributed to contaminants. This trend was much less marked for CS and absent or opposite for SS. Combining this observation with the contributions of the adlayer to the XPS spectrum, evaluated by $C_{tot} + C_{ox}$ (Table 4), suggests that glass, which initially carried a lower amount of surface contaminants, was able to pick up more proteins, compared to steel. However, questions remain regarding the respective fate of the contaminants and compounds introduced by conditioning, in particular regarding whether organic contaminants were displaced by the proteins of the conditioning solutions, or whether protein adsorption protected the sample from subsequent contamination in the ambient atmosphere, in the spectrometer vacuum chamber or during analysis. Further questions concern the possible layering of different constituents of the adlayer. This was addressed in the case of silane-grafted silicon wafers, a smooth substratum, by XPS analysis using two angles of photoelectron collection and indicated that the grafted layer of 1–2 nm thickness was covered with a monolayer of adventitious organic contaminants (Dekeyser et al. 2008).

Conclusions

By giving the concentrations of elements and chemical functions at the exposed surface, XPS provided information on the concentration of the main classes of biochemical compounds. This required peak decomposition, which involved reasonable constraints to ensure the consistency needed to make quantitative comparisons between samples, and was supported by correlations between independent spectral data. Most nitrogen was in the form of amide; the proportion which may be due to DNA was < 15% and was neglected. A convenient way of comparing different systems was to use ternary diagrams presenting the weight fraction of three model moieties: amide [HC-NH-(C=O)], CH_2, and the sum of additional organic oxygen and additional carbon in the oxidized form. This allowed the authors to cope with the adventitious contaminants present on non-conditioned materials and facilitated comparisons between samples.

Proteins or peptides were found to be a major constituent both at the surface of the evaporation residues and in the adlayers formed by conditioning the substrata with the EPS of *D. alaskensis* and *D. desulfuricans*, and with fresh or spent culture medium of *Pseudomonas* NCIMB 2021. Polysaccharides were not in appreciable concentration in the conditioning layer. At this level of characterization, there was no significant difference between the compositions of the adlayers formed from culture media and from solutions of extracted EPS. An exception was the adlayers produced with the TB-EPS extracted from *D. alaskensis*, which had a protein concentration higher than that of other systems. XPS has no selectivity regarding the nature of proteins and is not suitable to study the adsorption competition between different proteins (Nonckreman et al. 2010), which may possess different physico-chemical properties and offer different possibilities for specific interactions. However, the discrimination between classes of biochemical compounds may be useful for designing antifouling strategies, for instance for selecting enzymes which may prevent biofilm formation or to understand the loss of activity of grafted enzymes (Swartjes et al. 2013).

Conditioning the substrata only moderately increased the amount of organic compounds present at the surface, with respect to that found on non-conditioned substrata, which was due to the presence of adventitious contaminants. Differences between substrata thus largely result from competition between contaminants and biochemical compounds introduced by conditioning. This is a severe limitation for the comparison between experimental data and for basic concerns regarding bioadhesion, but is neglected in the literature.

Acknowledgements

The DNA samples were kindly provided by Michel Thiel (ELI-M, Université catholique de Louvain).

Disclosure statement

No potential conflict of interest was reported by the authors.

Funding

The support of Fonds National de la Recherche Scientifique (Belgium) and of Belspo (Interuniversity Attraction Poles Program) is gratefully acknowledged. This research was funded by the European Community Seventh Framework Programme (FP7/2007-2013) under grant agreement [no 238579] (Project website: www.biocor.eu/ip9).

References

Aguié-Béghin V, Adriaensen Y, Péron N, Valade M, Rouxhet P, Douillard R. 2009. Structure and chemical composition of layers adsorbed at interfaces with champagne. J Agric Food Chem. 57:10399–10407. DOI: 10.1021/jf9016948

Ahimou F, Boonaert CJP, Adriaensen Y, Jacques P, Thonart P, Paquot M, Rouxhet PG. 2007. XPS analysis of chemical functions at the surface of *Bacillus subtilis*. J Colloid Interface Sci. 309:49–55. DOI: 10.1016/j.jcis.2007.01.055

Beech IB, Gubner R, Zinkevich V, Hanjangsit L, Avci R. 2000. Characterisation of conditioning layers formed by exopolymeric substances of *Pseudomonas* NCIMB 2021 on surfaces of AISI 316 stainless steel. Biofouling. 16:93–104. DOI: 10.1080/08927010009378435

Beech I, Hanjagsit L, Kalaji M, Neal AL, Zinkevich V. 1999. Chemical and structural characterization of exopolymers produced by *Pseudomonas* sp. NCIMB 2021 in continuous culture. Microbiology. 145:1491–1497. DOI: 10.1099/13500872-145-6-1491

Beech IB, Zinkevich V, Tapper R, Gubner R. 1998. Direct involvement of an extracellular complex produced by a marine sulfate-reducing bacterium in deterioration of steel. Geomicrobiol J. 15:121–134. DOI: 10.1080/01490459809378069

Beech IB, Zinkevich V, Tapper R, Gubner R, Avci R. 1999. Study of the interaction of sulphate-reducing bacteria exopolymers with iron using X-ray photoelectron spectroscopy and time-of-flight secondary ionisation mass spectrometry. J Microbiol Methods. 36:3–10. DOI: 10.1016/S0167-7012(99)00005-6

Berne C, Kysela DT, Brun YV. 2010. A bacterial extracellular DNA inhibits settling of motile progeny cells within a biofilm. Mol Microbiol. 77:815–829. DOI: 10.1111/j.1365-2958.2010.07267.x

Boonaert CJP, Dufrêne YF, Rouxhet PG. 2002. Adhesion (primary) of microorganisms onto surfaces. In: Bitton G, editor, Encyclopedia of environmental microbiology. New York: Wiley; p. 113–132. DOI: 10.1002/0471263397.env154.

Bosquillon C, Rouxhet PG, Ahimou F, Simon D, Culot C, Préat V, Vanbever R. 2004. Aerosolization properties, surface composition and physical state of spray-dried protein powders. J Controlled Release. 99:357–367. DOI: 10.1016/j.jconrel.2004.07.022

Bradford MM. 1976. Rapid and sensitive method for the quantitation of microgram quantities of protein utilizing the principle of protein–dye binding. Anal Biochem. 72:248–254. DOI: 10.1016/0003-2697(76)90527-3

Burton K. 1956. A study of the conditions and mechanism of the diphenylamine reaction for the colorimetric estimation of deoxyribonucleic acid. Biochem J. 62:315–323. DOI: 10.1042/bj0620315

Conrad A, Kontro M, Keinänen M, Cadoret A, Faure P, Mansuy-Huault L, Block J-C. 2003. Fatty acids of lipid fractions in extracellular polymeric substances of activated sludge flocs. Lipids. 38:1093–1105. DOI: 10.1007/s11745-006-1165-y

Dall'Agnol LT, Cordas CM, Moura JJG. 2014. Influence of respiratory substrate in carbon steel corrosion by a sulphate reducing prokaryote model organism. Bioelectrochemistry. 97:43–51. DOI: 10.1016/j.bioelechem.2013.10.006

Dekeyser CM, Buron CC, Mc Evoy K, Dupont-Gillain CC, Marchand-Brynaert J, Jonas AM, Rouxhet PG. 2008. Oligo(ethylene glycol) monolayers by silanisation of silicon wafers: real nature and stability. J Colloid Interface Sci. 324:118–126. DOI: 10.1016/j.jcis.2008.05.002

Dubois M, Gilles KA, Hamilton JK, Rebers PA, Smith F. 1956. Colorimetric method for determination of sugars and related substances. Anal Chem. 28:350–356. DOI: 10.1021/ac60111a017

Dufrêne YF, Vermeiren H, Vanderleyden J, Rouxhet PG. 1996. Direct evidence for the involvement of extracellular proteins in the adhesion of *Azospirillum brasilense*. Microbiology. 142:855–865. DOI: 10.1099/00221287-142-4-855

Dyballa N, Metzger S. 2009. Fast and sensitive colloidal coomassie G-250 staining for proteins in polyacrylamide gels. J Vis Exp. 30:e1431. DOI: 10.3791/1431

Feio MJ, Zinkevich V, Beech IB, Llobet-Brossa E, Eaton P, Schmitt J, Guezennec J. 2004. *Desulfovibrio alaskensis sp.* nov., a sulphate-reducing bacterium from a soured oil reservoir. Int J Syst Evol Microbiol. 54:1747–1752.10.1099/ijs.0.63118-0

Flemming H-C. 2011. The perfect slime. Colloids Surf B Biointerfaces. 86:251–259. DOI: 10.1016/j.colsurfb 2011.04.025

Flemming H-C, Wingender J. 2003. Extracellular polymeric substances (EPS): structural, ecological and technical aspects. In: Bitton, G, editor. Encyclopedia of environmental microbiology. New York: Wiley. p. 1223–1231. DOI: 10.1002/0471263397.env292

Flemming H-C, Wingender J. 2010. The biofilm matrix. Nat Rev Microbiol. 8:623–633. DOI: 10.1128/CMR.15.2.167-193.2002

Frølund B, Palmgren R, Keiding K, Nielsen PH. 1996. Extraction of extracellular polymers from activated sludge using a cation exchange resin. Water Res. 30:1749–1758. DOI: 10.1016/0043-1354(95)00323-1

GE Healthcare. 2004. 2-D electrophoresis: principles and methods. GE Healthcare. Available from: http://www.gelifesciences.com/file_source/GELS/Service%20and%20Support/Documents%20and%20Downloads/Handbooks/pdfs/2-D%20Electrophoresis.pdf

Genet MJ, Dupont-Gillain CC, Rouxhet PG. 2008. XPS analysis of biosystems and biomaterials. In: Matijevic E, editor. Medical applications of colloids. New York: Springer; p. 177–307.

Gloag ES, Turnbull L, Huang A, Vallotton P, Wang H, Nolan LM, Mililli L, Hunt C, Lu J, Osvath SR, et al. 2013. Self-organization of bacteriel biofilms is facilitated by

exctracellular DNA. PNAS. 110:11541–11546. DOI: 10.1073/pnas.1218898110

Gómez-Suárez C, Pasma J, van der Borden AJ, Wingender J, Flemming H-C, Busscher HJ, van der Mei HC. 2002. Influence of extracellular polymeric substances on deposition and redeposition of *Pseudomonas aeruginosa* to surfaces. Microbiology. 148:1161–1169. DOI: 10.1099/00221287-148-4-1161

Graham DJ, Midgley NG. 2000. Graphical representation of particle shape using triangular diagrams: an Excel spreadsheet method. Earth Surf Process Landf. 25:1473–1477. DOI: 10.1002/1096-9837(200012)25:13<>1.0.CO;2-D

Hwang G, Kang S, El-Din MG, Liu Y. 2012a. Impact of conditioning films on the initial adhesion of *Burkholderia cepacia*. Colloids Surf B Biointerfaces. 91:181–188. DOI: 10.1016/j.colsurfb.2011.10.059

Hwang G, Kang S, El-Din MG, Liu Y. 2012b. Impact of an extracellular polymeric substance (EPS) precoating on the initial adhesion of *Burkholderia cepacia* and *Pseudomonas aeruginosa*. Biofouling. 28:525–538. DOI: 10.1080/08927014.2012.694138

Hwang G, Liag J, Kang S, Tong M, Liu Y. 2013. The role of conditioning film formation in *Pseudomonas aeruginosa* PAO1 adhesion to inert surfaces in aquaric environments. Biochem Eng J. 76:90–98. DOI: 10.1016/j.bej.2013.03.024

Jain A, Bhosle NB. 2009. Biochemical composition of the marine conditioning film: implications for bacterial adhesion. Biofouling. 25:13–19. DOI: 10.1080/08927010802411969

Jakubovics NS, Shields RC, Rajarajan N, Burgess JG. 2013. Life after death: the critical role of extracellular DNA in microbial biofilms. Lett Appl Microbiol. 57:467–475. DOI: 10.1111/lam.2013.57.issue-6

KarkhanisYD, Zeltner JY, Jackson JJ, Carlo DL. 1978. A new and improved microassay to determine 2-keto-3-deoxy-octonate in lipopolysaccharide of Gram-negative bacteria. Anal Biochem. 85: 595–601. DOI: 10.1016/0003-2697(78)90260-9

Laemmli UK. 1970. Cleavage of structural proteins during the assembly of the head of bacteriophage T4. Nature. 227:680–685. DOI: 10.1038/227680a0

Landoulsi J, Genet MJ, Richard C, El Kirat K, Pulvin S, Rouxhet PG. 2008. Evolution of the passive film and organic constituents at the surface of stainless steel immersed in fresh water. J Colloid Interface Sci. 318:278–289. DOI: 10.1016/j.jcis.2007.09.087

Landoulsi J, Genet MJ, El Kirat K, Richard C, Pulvin S, Rouxhet PG. 2011. Silanization with APTES for controlling the interactions between stainless steel and biocomponents: reality *vs* expectation. In: Pignatello R, editor. Biomaterials – Physics and Chemistry. Rijeka: Intech Open Access; p. 99–126.

Neihof R, Loeb G. 1974. Dissolved organic matter in seawater and the electric charge of immersed surfaces. J Mar Res. 32:5–12.DOI: 10.4319/lo.1995.40.4.0802/pdf

Neu TR, Marshall KC. 1991. Microbial "footprints" – A new approach to adhesive polymers. Biofouling. 3:101–112.10.1080/08927019109378166

Nonckreman CJ, Fleith S, Rouxhet PG, Dupont-Gillain CC. 2010. Competitive adsorption of fibrinogen and albumin and blood platelet adhesion on surfaces modified with nanoparticles and/or PEO. Colloids Surf B Biointerfaces. 77:139–149. DOI: 10.1016/j.colsurfb.2010.01.014

Rouxhet PG. 2013. Contact angles and surface energy of solids: relevance and limitations. In: Mittal KL, editor. Advances in contact angle, wettability and adhesion. Beverly, MA: Scrivener, Vol 1, Ch. 20; p. 349–375.

Rouxhet PG, Genet MJ. 2011. XPS analysis of bio-organic systems. Surf Interface Anal. 43:1453–1470. DOI: 10.1002/sia.v43.12

Rouxhet PG, Misselyn-Bauduin AM, Ahimou F, Genet MJ, Adriaensen Y, Desille T, Bodson P, Deroanne C. 2008. XPS analysis of food products: toward chemical functions and molecular compounds. Surf Interface Anal. 40:718–724. DOI: 10.1002/(ISSN)1096-9918

Schneider RP, Leis A. 2003. Conditioning films in aquatic environments. In: Bitton G, editor. Encyclopedia of environmental microbiology. New York: Wiley; p. 928–941. DOI: 10.1002/0471263397.env036.

Stadler R, Wei L, Fürbeth W, Grooters M, Kuklinski A. 2010. Influence of bacterial exopolymers on cell adhesion of *Desulfovibrio vulgaris* on high alloyed steel: corrosion inhibition by extracellular polymeric substances (EPS). Mater Corros. 61:1008–1016. DOI: 10.1002/maco.v61.12

Swartjes JJTM, Das T, Sharifi S, Subbiahdoss G, Sharma PK, Krom BP, Busscher HJ, van der Mei HC. 2013. A functional DNase coating to prevent adhesion of bacteria and the formation of biofilm. Adv Funct Mater. 23:2843–2849. DOI: 10.1002/adfm.201202927

Torres Bautista BE, Wikiel AJ, Datsenko I, Vera M, Sand W, Seyeux A, Zanna S, Frateur I, Marcus P. 2015. Influence of extracellular polymeric substances (EPS) from *Pseudomonas* NCIMB 2021 on the corrrosion behaviour of 70Cu30Ni alloy in seawater. J Electroanal Chem. 737:184–197. DOI: 10.1016/j.jelechem.2014.09.024

Touré Y, Genet MJ, Dupont-Gillain CC, Sindic M, Rouxhet PG. 2014. Conditioning materials with biomacromolecules: composition of the adlayer and influence on cleanability. J Colloid Interface Sci. 432:158–169. DOI: 10.1016/j.jcis.2014.06.002

Whitchurch CB, Tolker-Nielsen T, Ragas PC, Mattick JS. 2002. Extracellular DNA required for bacterial biofilm formation. Science. 295:1487. DOI: 10.1126/science.295.5559.1487

Wingender J, Strathmann M, Rode A, Leis A, Flemming H-C. 2001. Isolation and biochemical characterization of extracellular polymeric substances from *Pseudomonas aeruginosa*. Methods Enzymol. 336:302–314. DOI: 10.1016/S0076-6879(01)36597-7

Yuan SJ, Pehkonen SO. 2007. Microbiologically influenced corrosion of 304 stainless steel by aerobic *Pseudomonas* NCIMB 2021 bacteria: AFM and XPS study. Colloids Surf B Biointerfaces. 59:87–99. DOI: 10.1016/j.colsurfb.2007.04.020

Zinkevich V, Beech IB. 2000. Screening of sulfate-reducing bacteria in colonoscopy samples from healthy and colitic human gut mucosa. FEMS Microbiol Ecol. 34:147–155. DOI: 10.1111/fem.2000.34.issue-2

Zinkevich V, Bogdarina I, Kang H, Hill MAW, Tapper R, Beech IB. 1996. Characterisation of exopolymers produced by different isolates of marine sulphate-reducing bacteria. Int Biodeterior Biodegrad. 37:163–172. DOI: 10.1016/S0964-8305(96)00025-X